Classification: BIOLOGICAL SCIENCES; Neuroscience.

Title: TIA1 potentiates tau phase separation and promotes generation of toxic oligomeric tau

Authors:

Peter E.A. Ash[a, j], Shuwen Lei[a, j], Jenifer Shattuck[a], Samantha Boudeau[a], Yari Carlomagno[b], Maria Medalla[c, g], Bryce L. Mashimo[a], Guillermo Socorro[a], Louloua F.A. Al-Mohanna[a], Lulu Jiang[a], Muhammet M. Öztürk[a], Mark Knobel[a], Pavel Ivanov[d], Leonard Petrucelli[b], Susanne Wegmann[e], Nicholas M. Kanaan[f], Benjamin Wolozin[a, g, h, l, *].

Author Affiliations:

[a] Department of Pharmacology and Experimental Therapeutics, Boston University School of Medicine, 72 East Concord Street, Boston, MA. 02118. USA.

[b] Department of Neuroscience, Mayo Clinic Florida, 4500 San Pablo Road, Jacksonville, FL. 32224, USA.

[c] Department of Anatomy and Neurobiology, Boston University School of Medicine, 72 East Concord Street, Boston, MA. 02118. USA.

[d] Division of Rheumatology, Immunology and Allergy, Brigham and Women's Hospital, Harvard Medical School, Boston, Massachusetts 02115, USA.

[e] German Center for Neurodegenerative Diseases (DZNE), Berlin, Germany.

[f] Department of Translational Neuroscience, Michigan State University, Grand Rapids Research Center, 400 Monroe Ave. NW, Grand Rapids, MI. 49503. USA.

[g] Department of Neurology, [h] Center for Systems Neuroscience, and [i] The Neurophotonics Center, Boston University School of Medicine, 72 East Concord Street, Boston, MA. 02118. USA.

[j] These authors contributed equally.

* Correspondence should be addressed to bwolozin@bu.edu, 617-358-1995.

Orchid IDs:

Peter Ash: 0000-0002-9557-3674

Benjamin Wolozin: 0000-0003-2068-1475

Susanne Wegmann: 0000-0002-5388-2479

Nicholas M. Kanaan: 0000-0002-4362-2593

SI Appendix

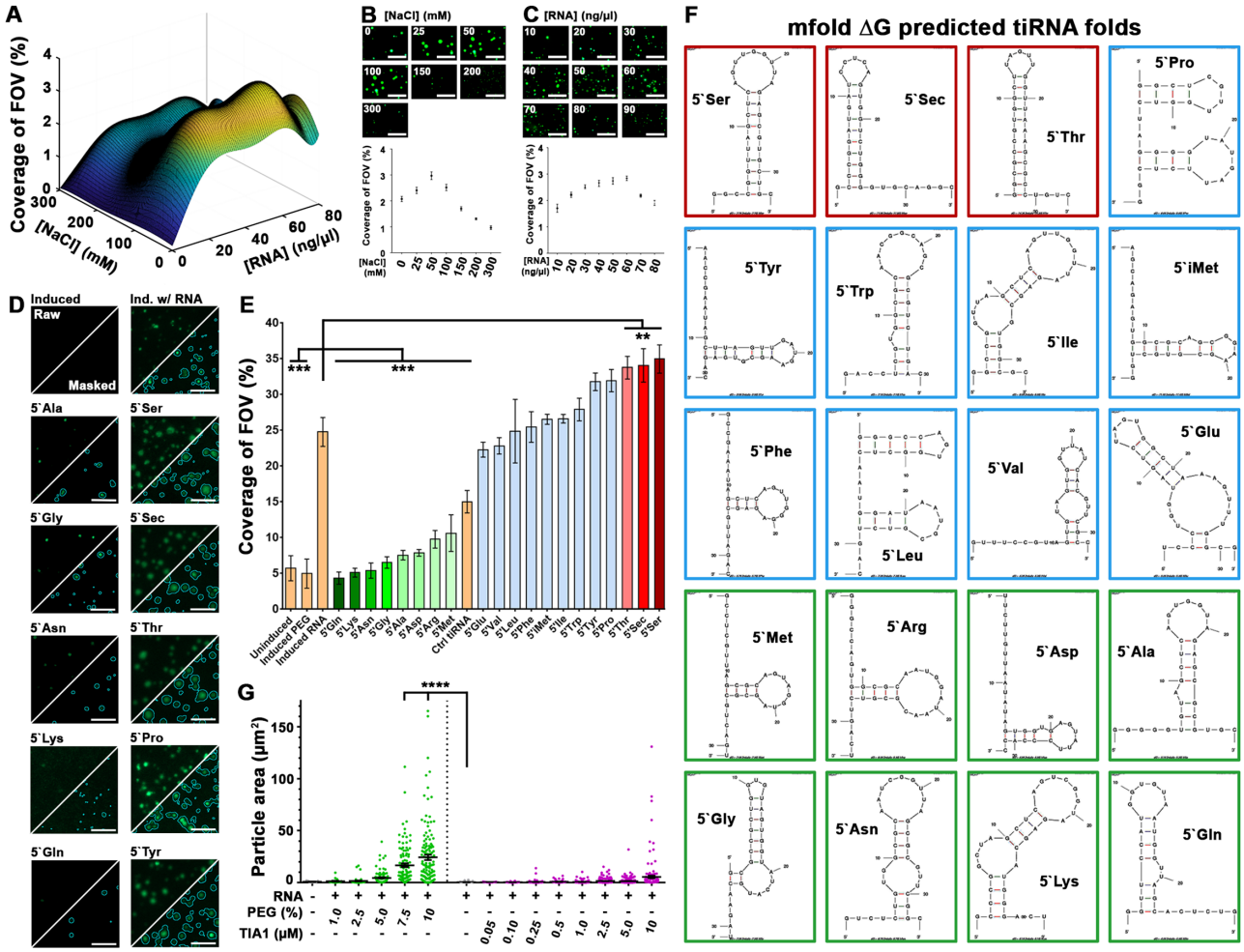

SI Appendix Fig. S1: A) Optimal phase separation of 0N4R wild type tau (5µM) occurs in 50mM NaCl with 60ng/µl total murine brain RNA and 10% PEG-8000. **B)** Optimization of NaCl concentration in 10% PEG-induced LLPS of 0N4R wild type tau-488 (5µM). **C)** Optimization of total murine brain RNA concentration in 10% PEG-induced LLPS of 0N4R wild type tau-488 (5µM). Scale bars = 5µm. **D)** Phase separation of 0N4R wild type tau-488 in the presence of 20ng/µl total RNA or 10µM tiRNAs (fluorescent images in top left, with ImageJ mask overlay in bottom left). **E)** Quantification of 0N4R wild type tau-488 phase separation in the presence of tiRNAs. (***P < 0.001, **P < 0.01. N = 5/group, mean ± SEM, ANOVA w/ Dunnetts post-hoc comparison against uninduced control). **F)** Predicted folding of tiRNAs used in tau LLPS reactions in panels D and E. Folds are predicted by mfold web server (http://unafold.rna.albany.edu/?q=mfold) based on minimum free energy, ΔG. Compared to total brain RNA, red border: tiRNAs inducing significant increase in tau LLPS; blue border = non-significant; green border = significantly less tau LLPS induced. **G)** Quantification of tau-488 droplet formation in presence of TIA1 as area of particles formed. (****P < 0.0001, N = 5/group, mean ± SEM, ANOVA w/ Dunnetts post-hoc comparison against RNA only group).

Co-phase separation of tau/RBP

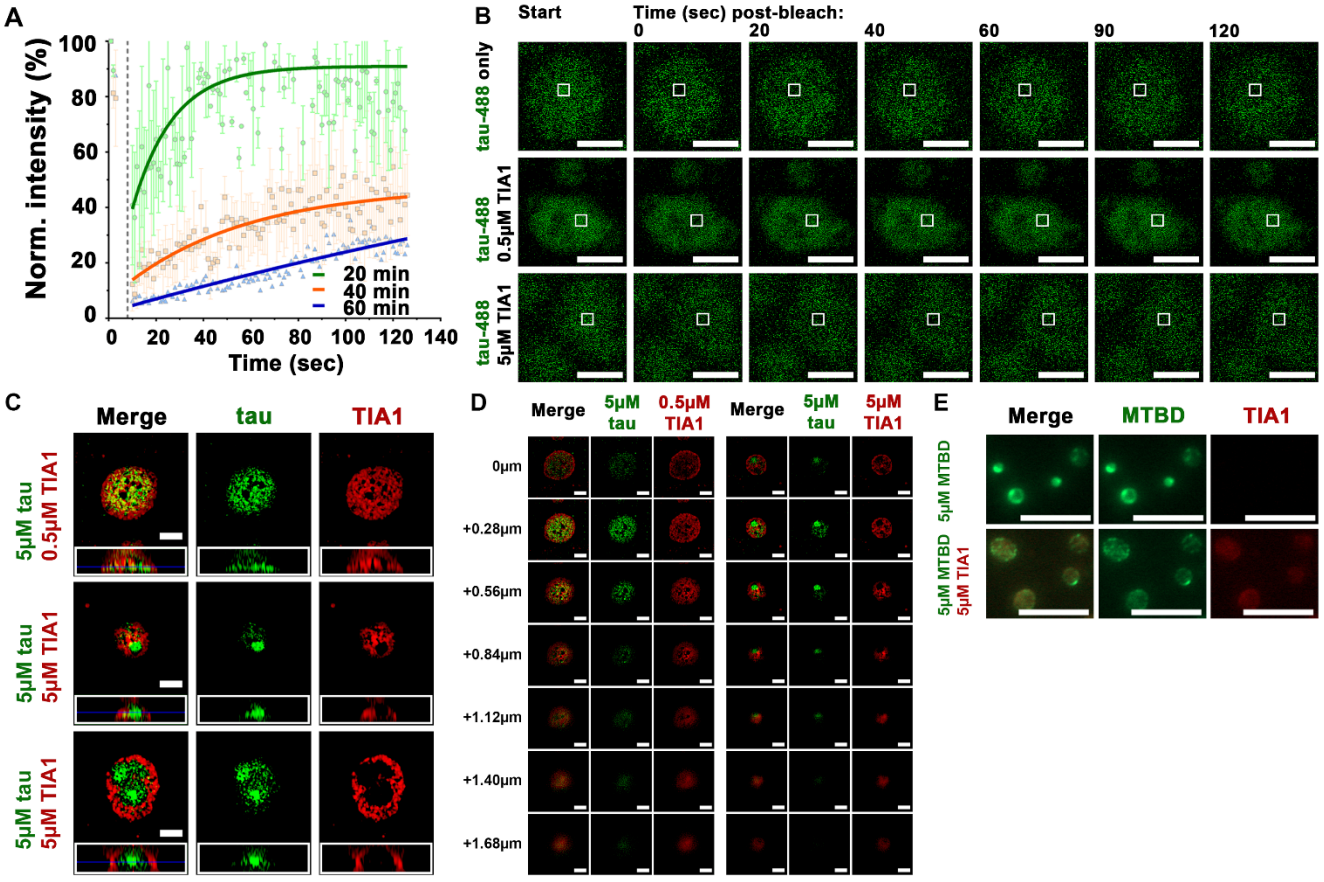

SI Appendix Fig. S2: A) With increasing incubation time, phase separated tau shows reduced recovery after photobleaching, indicating time-dependent gelation (decreased fluidity). Phase separated tau-488 was assessed by FRAP 20, 40 or 60 minutes after induction with 10% PEG and 20ng/μl RNA. **B)** Representative time-series images of FRAP experiment in Figure S2A. White box is area of bleaching and imaging. **C)** Orthogonal maximum intensity projection image from structured illumination microscopy of tau-488 phase separation in presence of TIA1-594. **D)** Gallery view of SIM z-stack of tau-DL488 within TIA1-DL594 droplets. Coverslip is at top (~0μM). Images used in orthogonal MIP image in Supp. Figure S2C. Scale bars for B, C, and D = 2μm. **E)** MTBD-488 phase separates into diffuse droplets even in the presence of TIA1-594, suggesting that while this domain efficiently undergoes phase separation, other domains are necessary for microdomain formation. Scale bar 10μm.

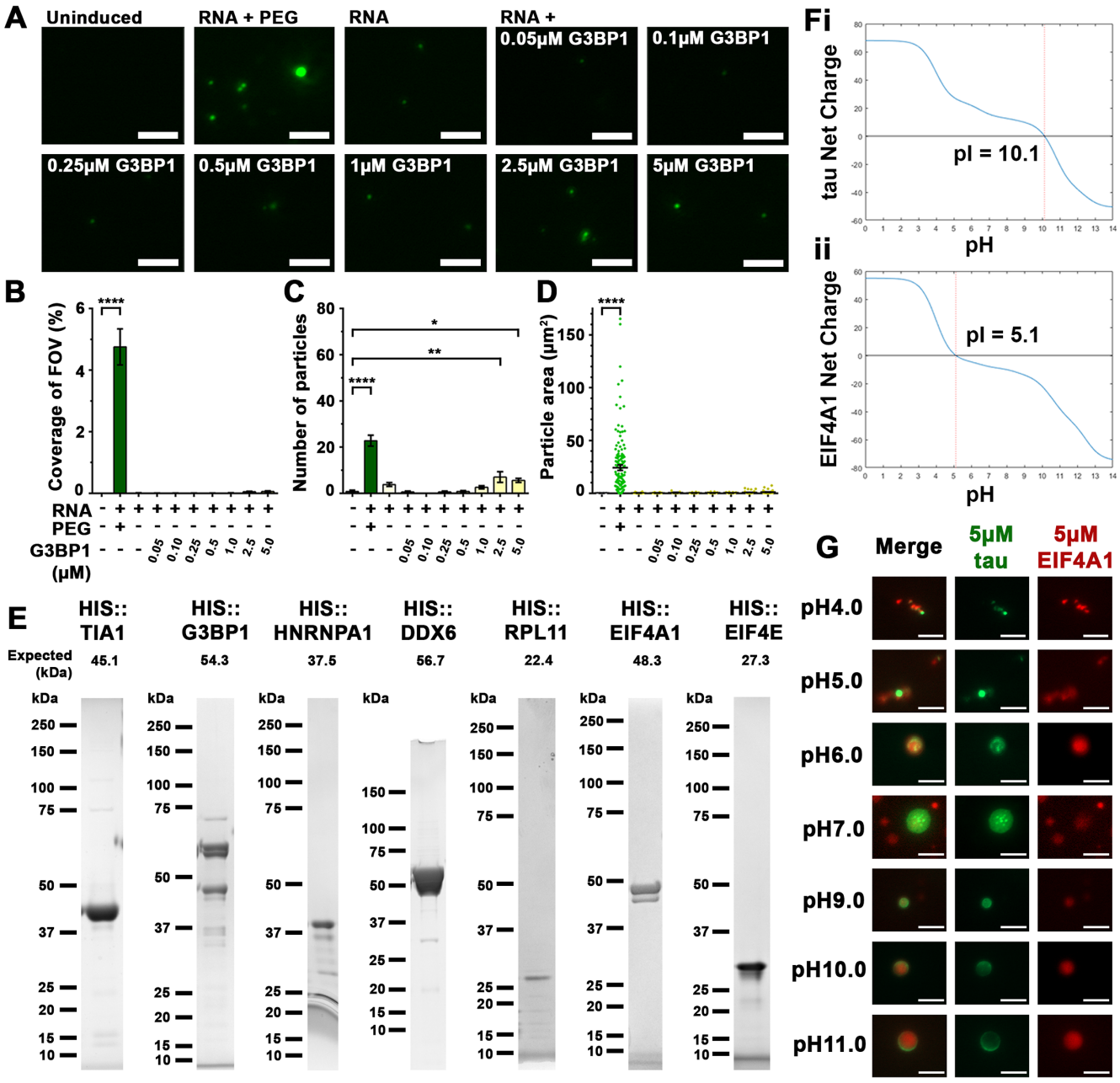

SI Appendix Fig. S3: A) G3BP1 can substitute for PEG to facilitate phase separation of tau-488, however, not as efficiently as TIA1. **B)** Quantification of tau-488 droplet formation in presence or G3BP1 as coverage of field of view. **C)** Quantification of tau-488 droplet formation in presence or G3BP1 as number of particles formed. **D)** Quantification of tau-488 droplet formation in presence of G3BP1 as area of particles formed. (For B, C, and D: **P* < 0.05, ***P* < 0.01, *****P* < 0.0001. N = 5/group, mean ± SEM, ANOVA w/ Dunnetts post-hoc comparison against RNA only group). **E)** Coomassie stained BisTris NuPAGE gels showing HiTrap cobalt chelating/HiPrep size-exclusion-chromatography purified recombinant HIS fused RBPs used in this study. **F)** Predicted net charge of tau (i) and EIF4A1 (ii) across pH range, with pIs of 10.1 and 5.1 respectively. **G)** Partitioning pattern of tau-488 (5μM) and EIF4A1-594 (5μM) are pH dependent. Scale bars 5μm.

Co-phase separation of tau/RBP

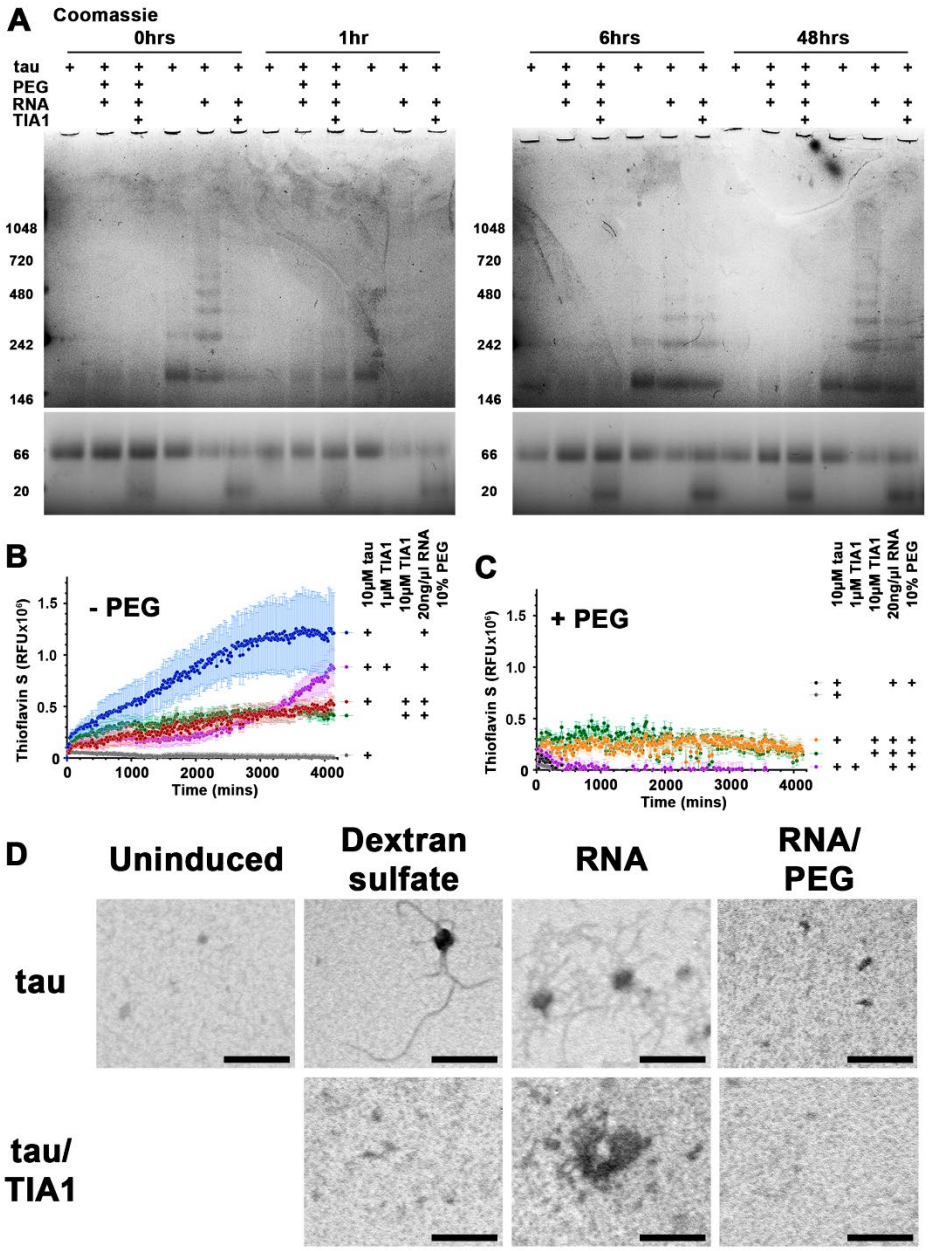

SI Appendix Fig. S4: A) NativePAGE with Coomassie showing time course (0, 1, 6 and 48 hours) of tau multimerization in reactions mixed ± PEG, RNA and/or TIA1. **B)** Thioflavin S (ThS) fluorescent assay shows robust formation of amyloid when induced with RNA. Addition of 1μM TIA1, delays accumulation of ThS positive amyloids in RNA-induced tau, while 10μM TIA1 blocked ThS accumulation over the duration of the experiment. **C)** ThS fluorescent assay shows no formation of amyloid in PEG/RNA induced droplets of liquid tau. No amyloid forms upon addition of 1μM or 10μM TIA1, which produces vitrified tau. (RFU relative fluorescent units). **D)** Transmission electron microscopy images of 10μM 0N4R wild type tau. Dextran sulfate (0.04mg/ml) and RNA (20ng/μl) induce formation of fibrils. Addition of TIA1 or PEG prevent fibrillization of tau. Scale bars 200nm.

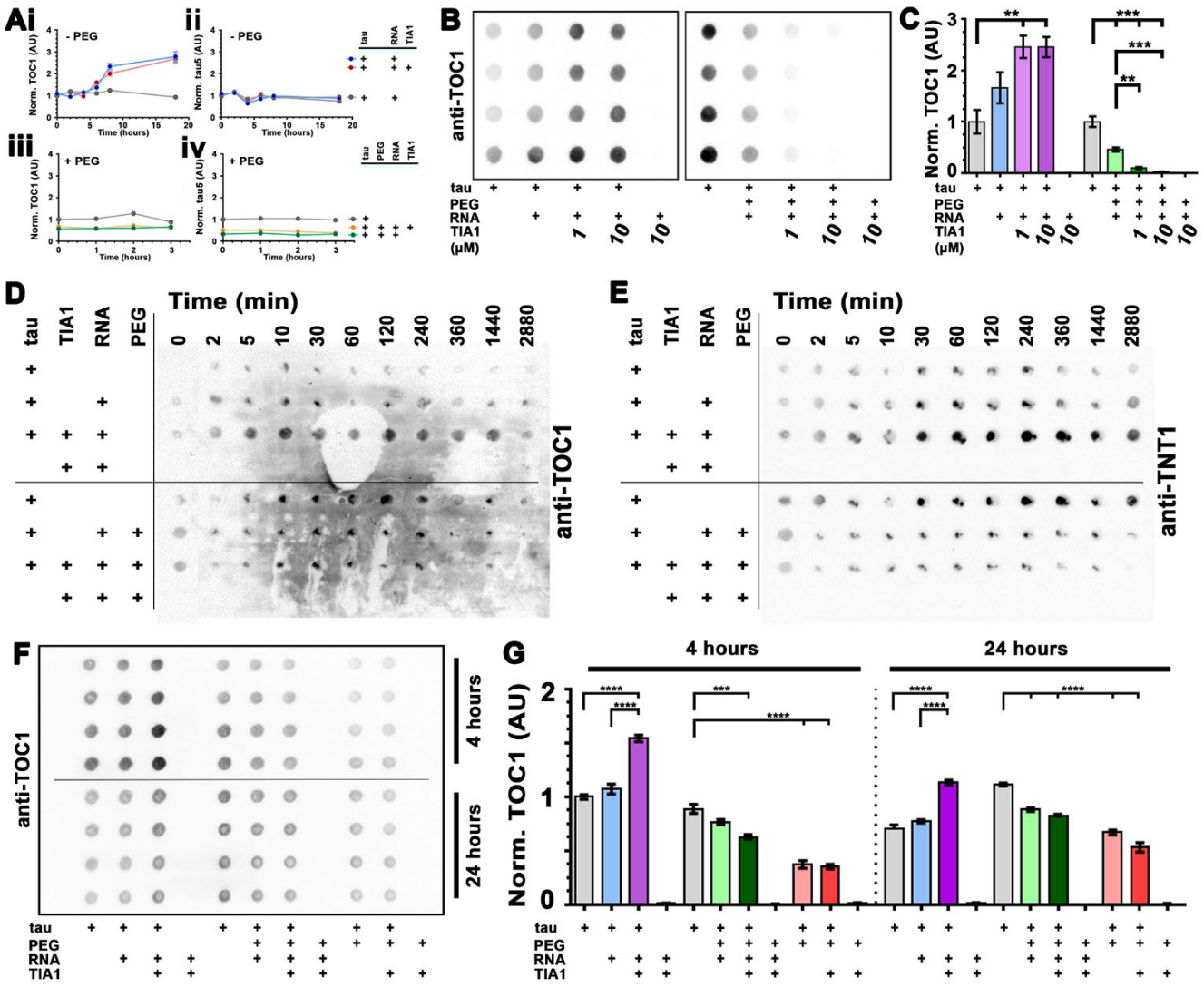

SI Appendix Fig. S5: Ai) TOC1 ELISAs show an increase in tau oligomers in RNA-induced tau and RNA/TIA1-induced tau samples compared to uninduced control over a 24 hour time course. **ii)** tau5 ELISAs for normalization of TOC1 ELISA in panel i. **iii)** TOC1 ELISAs of uninduced, PEG/RNA-induced tau and PEG/RNA/TIA1-induced tau shows no accumulation of tau oligomers over 3 hours. **iv)** tau5 ELISAs for normalization of TOC1 ELISA in panel iii. (For D: AU arbitrary units. N = 3/group, mean ± SEM). **B)** Dot blots of samples (used for ELISAs in Figure 3D) immunolabelled with anti-oligomeric tau antibody TOC1. **C)** Quantification of dot densitometry (from panel E) shows that in the presence of RNA and TIA1 (either 1μM or 10μM), tau undergoes significant oligomerization. PEG-induced tau, ±TIA1, has significantly less TOC1 reactivity than uninduced control. **D)** Dot blot immunolabelled with TOC1 shows that over a 48 hour time period, RNA/TIA1-induction of tau leads to accumulation of TOC1-positive oligomeric tau. However, PEG/RNA-induced tau and PEG/RNA/TIA1-induced tau exhibits decreasing oligomeric tau over the experimental time period. **E)** A similar trend is observed upon dot blot and immunolabelling with TNT, which recognizes a conformational alteration in tau. **F)** Dot blots of tau

samples incubated for 4 or 24 hours, immunolabelled with TOC1 anti-oligomeric tau antibody. **G)** Quantification of dot densitometry (from panel I) shows that in the presence of TIA1 (and RNA), tau undergoes significant oligomerization. PEG-induced tau, ±TIA1, ±RNA, shows no change, or significantly less TOC1 reactivity than uninduced control. (For F and J: AU arbitrary units. N = 4/group, mean ± SEM. *P < 0.05, **P < 0.01, ***P < 0.001, ****P < 0.0001. ANOVA w/ Tukey's post-hoc comparison between all groups).

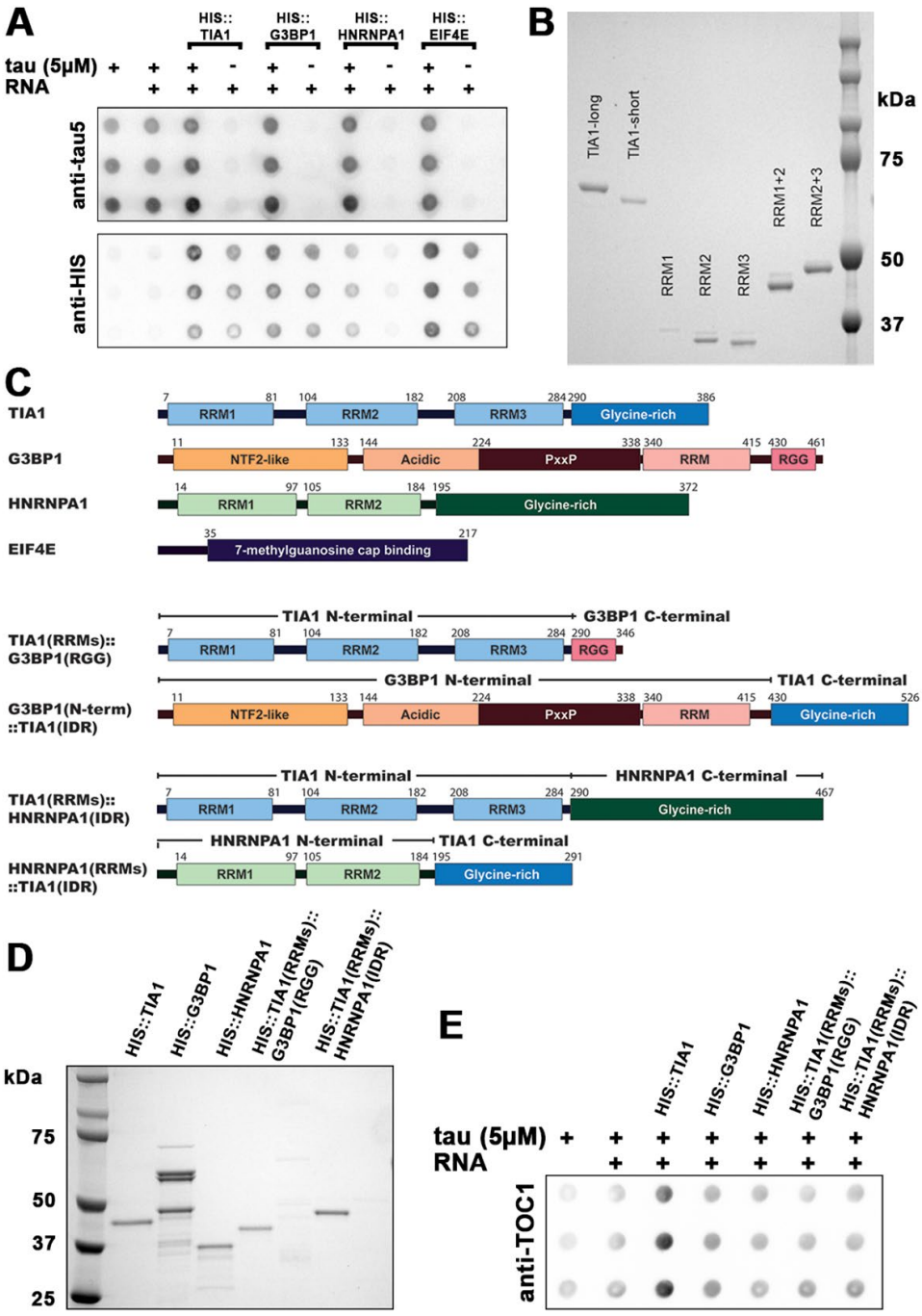

SI Appendix Fig. S6: A) Dot blots used in Figure 3G reprobed for total tau (tau5) and HIS-tagged RBPs. **B)** GST-tagged TIA1 and domains separated by SDS-PAGE and stained by coomassie. **C)** Schematic representation of TIA1, G3BP1 and HNRNPA1 domains and substituted domains in RBP hybrids HIS::TIA1(RRMs)::G3BP1(RGG), HIS::G3BP1(N-term)::TIA1(IDR), HIS::TIA1(RRMs)::HNRNPA1(IDR) and HIS::HNRNPA1(RRMs)::TIA1(IDR). **D)** Equal amounts of HIS-tagged RBPs and hybrid RBPs separated by SDS-PAGE and stained by coomassie. HIS::G3BP1(N-term)::TIA1(IDR) and HIS::HNRNPA1(RRMs)::TIA1(IDR) hybrid RBPs failed to express. **E)** TOC1 labelled dot blot of tau samples incubated with HIS-tagged RBPs and hybrid RBPs used for quantification in Figure 3K.

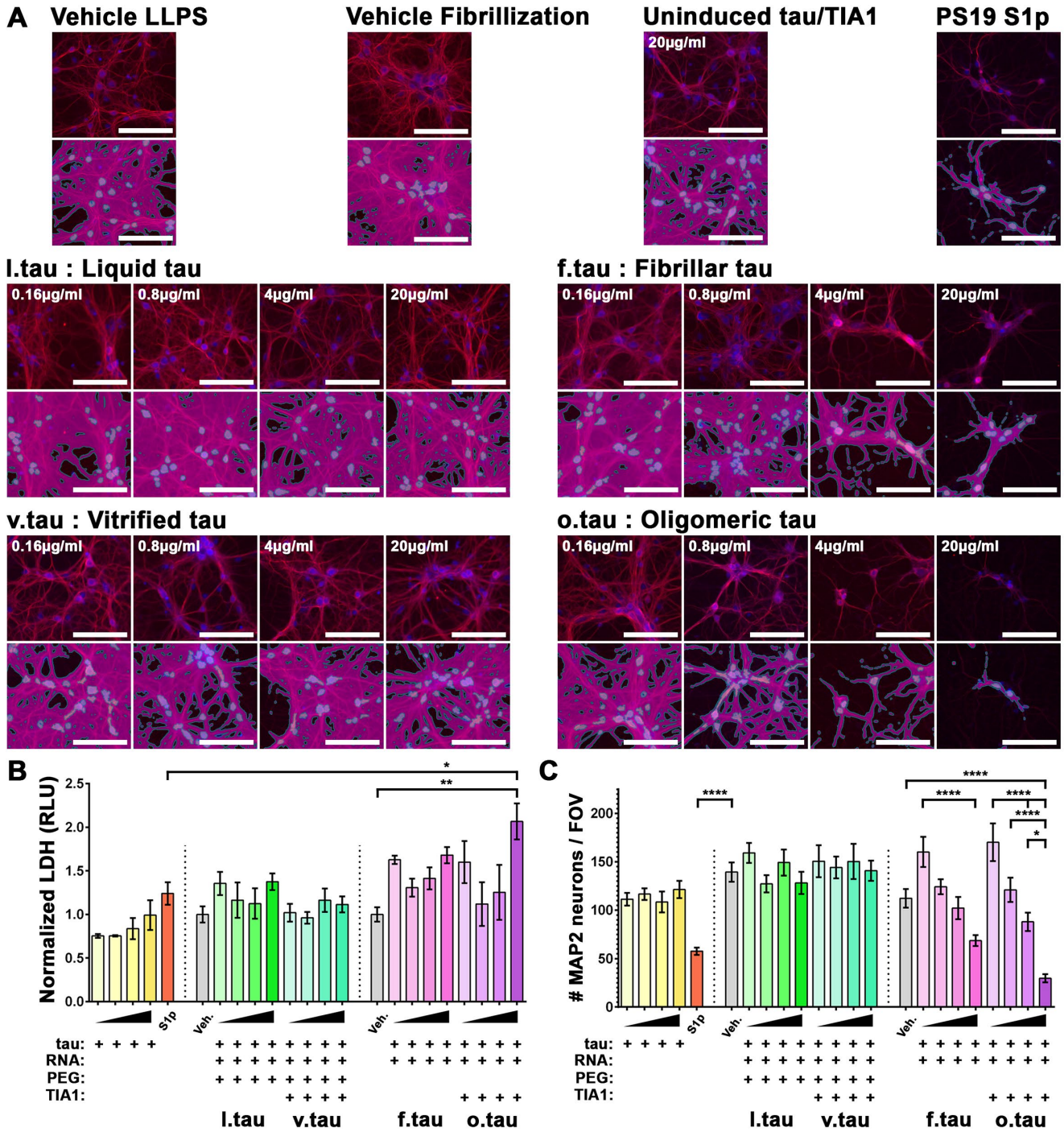

SI Appendix Fig. S7: A) Primary hippocampal neurons were treated for 7 days (DIV7 to 14) with liquid tau (**l.tau**), vitrified tau (**v.tau**), fibrillar tau (**f.tau**) and oligomeric tau (**o.tau**) at tau concentrations of 0.16µg/ml, 0.8µg/ml, 4µg/ml or 20µg/ml. Neurons were fixed (DIV14), stained for MAP2 (red) and counterstained with DAPI (blue) (top panels). Below each image is the mask for counting MAP2 positive neurons. Scale bar 100µm. **B)** Quantification of LDH release from primary neurons show that o.tau treatment causes neuronal toxicity at the highest concentration of 20µg/ml (RLU relative luminescent units). **C)** Quantification of MAP2-positive neuron

count shows that, compared to the vehicle control (grey bar), oligomeric tau (**o.tau**) treatment causes neuronal death. 20µg/ml o.tau treatment caused significantly greater loss of MAP2-positive neurons than treatment with either 0.16µg/ml, 0.8µg/ml or 4µg/ml o.tau. In comparison, treatment with fibrillar tau (**f.tau**) did not result in significantly greater loss of MAP2-positive neurons compared to the vehicle control (grey bar). 20µg/ml f.tau treatment caused significantly greater loss of MAP2-positive neurons than treatment with 0.16µg/ml f.tau. (For B and C: N = 3/group, mean ± SEM. *P < 0.05, **P < 0.01, ****P < 0.0001. ANOVA w/ Tukey's post-hoc comparison between all groups).

Table 1

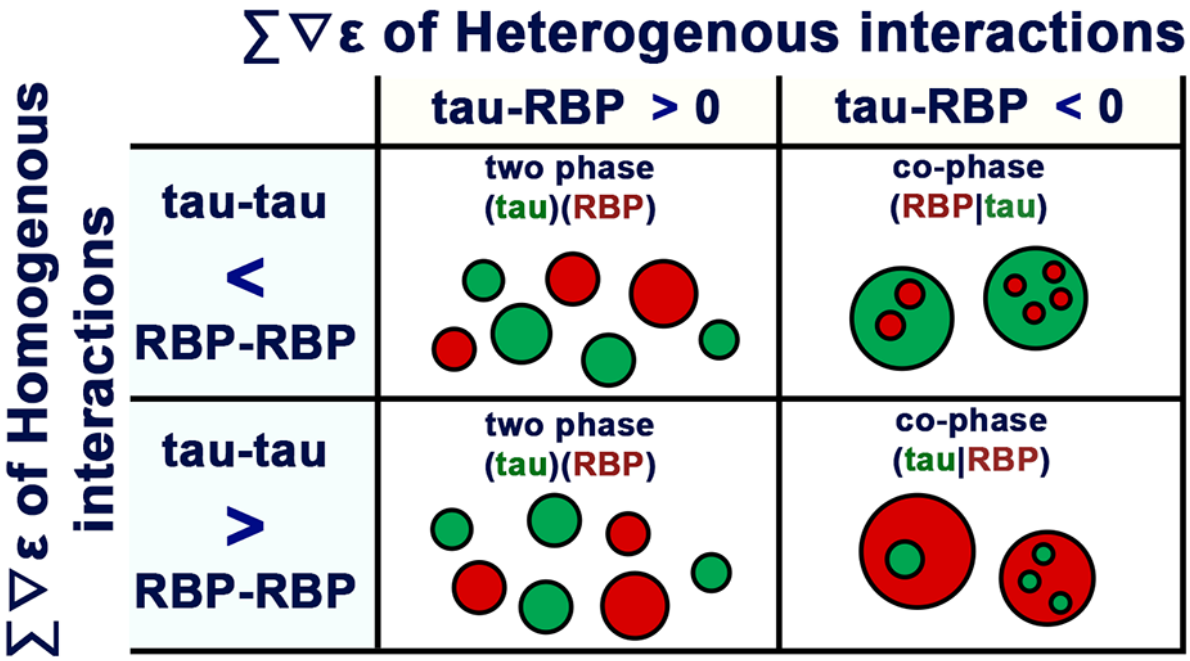

SI Appendix Table S1: Protein condensate partitioning behavior is predicted by the enthalpic gain (summed tensor field, Σ∇ε) generated by heterogeneous and homogeneous interactions within a system. Heterogeneous interactions that are energetically favorable (Σ∇ε tau-RBP < 0) result in co-phase separation of protein species; here (RBP|tau) and (tau|RBP). Further partitioning of a protein within droplets of another is a product of the relative gain in enthalpy from homogeneous interactions of each protein species.

SI Appendix material and methods:

Recombinant proteins preparation

4L to 8L of LB was inoculated from 20ml overnight cultures, grown at 37°C for ~3 hours to A_{600} ~0.5 then switched to 16°C, induced with 0.5mM IPTG and grown overnight. Bacteria from 4L culture were pelleted, resuspended in RBP buffer A (10mM HEPES pH7.4, 300mM NaCl, 10mM Imidazole) containing 2mM $MgCl_2$, 32μg/ml Lysozyme (Sigma), 4μg/ml DNaseI, 200μM PMSF and a tablet of protease inhibitor cocktail (Pierce). Bacteria were lysed 6 times in liquid N_2 and a tepid water bath. The lysate was clarified by centrifugation at 10,000rcf for 10 mins, diluted to ~250ml in lysis Buffer A then loaded by circulating pump to a cobalt chloride-charged, Buffer A equilibrated HiTrap HP Chelating column (GE). The column was then washed and eluted using an AKTApure FPLC (GE) using a gradient of Buffer A and RBP Buffer B (10mM HEPES pH7.4, 1M NaCl, 300mM Imidazole). Eluted RBPs were further purified by HiPrep 26/60 S-200 size exclusion column (GE) in RBP Storage Buffer (10mM HEPES pH7.4, 300mM NaCl, 5% Glycerol) then concentrated by Amicon Ultra-15 centrifugal filters (EMD). Recombinant proteins where aliquoted, snap frozen and stored at -80°C until use.

Use of the term "μM" refers to the molarity equivalent to monomeric tau; as tau changes aggregation state the actual molarity will vary according to the degree of aggregation. The same concept applies to other recombinant proteins used in this study.

Quantification of droplets and microdomains

To quantify size distribution and number of particles, we utilized the "Analyze Particle" built-in function in ImageJ with the auto threshold as "Standard". For calculating total droplet area, a logic variable is first determining by Matlab, which assigns the largest droplet area in the image by comparing different channels. If the logic variable is "1", then the red channel has the largest droplet area; if the logic variable is "0", then the green channel has the largest droplet area. The total area of RBP and tau droplets is then determined by summing the total area of the binarized matrix. The percentage of coverage first determines the degree of the pixel of crosstalk between the two binarized channel matrixes. Three blinded individuals scored percent microdomain formation from images taken from three independent LLPS experiments. For each channel (tau-488 and RBP-594), a score of 0 (all protein signal in droplet is diffuse) to 100 (all protein signal is in microdomains) was assigned. Hence, a microdomains score of 50% tau-488 and 0% RBP-594 would mean half of the tau protein is diffuse and half is in microdomains, while all of the RBP protein is in diffuse droplets. Graphing and statistical comparisons were performed as indicated in GraphPad Prism.

tiRNA induction of tau LLPS

Co-phase separation of tau/RBP

tiRNAs were purchased from IDT with 5' Phosphorylation with the following sequences (33): Ctrl1 5`Phos/UGAAGGGUUUUUUGUGUCUCUAUUUCCUUC; Ctrl2 5`Phos/UGU GAG UCA CGU GAG GGC AGA AUC UGC UC; Ctrl3 5`Phos/GCA UUC ACU UGG AUA GUA AAU CCA AGC UGA A; 5'Ala 5`Phos/GGG GGU GUA GCU CAG UGG UAG AGC GCG UGC; 5'Asn 5`Phos/GUC UCU GUG GCG CAA UCG GUU AGC GCG UUC GGC; 5'Asp 5`Phos/UUC UUG UUA AUA UAG UGG UGA GUA UUC CCA CC; 5'Arg 5`Phos/GGG CCA GUG GCG CAA UGG AUA ACG CGU CUG ACU; 5'Gly 5`Phos/GCG CCG CUG GUG UAG UGG UAU CAU GCA AGA U; 5'Gln 5`Phos/GGU UCC AUG GUG UAA UGG UUA GCA CUC UG; 5'Glu 5`Phos/UCC CUG GUA GUC UAG UGG CUA AAG UUU GGC G; 5'Ile 5`Phos/GGC CGG UUA GCU CAG UUG GUU AGA GCG UGG CGC; 5'iMet 5`Phos/AGC AGA GUG GCG CAG CGG AAG CGU GCU GG; 5'Lys 5`Phos/GCC CGG CUA GCU CAG UCG GUA GAG CAU GGG ACU; 5'Leu 5`Phos/GGG CCA GUG GCU CAA UGG AUA AUG CGU CUG AC; 5'Met 5`Phos/GCC UCG UUA GCG CAG UAG GUA GCG CGU CAG U; 5'Phe 5`Phos/GCC GAA AUA GCU CAG UUG GGA GAG CGU UAG AC; 5'Pro 5`Phos/GGC UCG UUG GUC UAG GGG UAU GAU UCU CGG; 5'Sec 5`Phos/GCC CGG AUG AUC CUC AGU GGU CUG GGG UGC AGG C; 5'Ser 5`Phos/GGC CGG UUA GCU CAG UUG GUU AGA GCG UGC UGC; 5'Thr 5`Phos/GGC GCC GUG GCU UAG UUG GUU AAA GCG CCU GUC; 5'Trp 5`Phos/GAC CUC GUG GCG CAA CGG CAG CGC GUC UGA C; 5'Tyr 5`Phos/AAC CGA AUA GCU UAG UUG AUG AAG CGU GAG AC; 5'Val 5`Phos/GUU UCC GUA GUG UAG UGG UUA UCA CGUUCG CC.

tau LLPS reactions were performed as above but using 2% PEG and 10µM tiRNA as indicated. Prediction of tiRNA secondary structure was performed using mfold web server (37) and are based on minimum free energy, ΔG.

Transmission Electron Microscopy (TEM) for visualization of tau fibrils

Reactions of tau (10µM) were incubated for 6 hours at 37°C in 10mM HEPES, pH7.4, 100mM NaCl, 1mM DTT and, where indicated, with 0.04mg/ml dextran sulfate, 20ng/µl RNA, 10% PEG-8000 and 10µM HIS::TIA1 (8). Following incubation, reactions were snap frozen on dry ice. Mixes were adsorbed for 2 min onto formvar/carbon-coated Copper mesh grids (EMS), washed 2x with distilled water (dH_20), treated with 2% uranyl acetate, washed 4x with dH_20. Grids were imaged at 50,000x magnification, 80 kV using a JEOL JEM 1011 with a digital camera (Gatan). About 10 random fields per sample were systematically sampled and imaged to verify for the presence of tau aggregates and fibrils.

Super-resolution microscopy

Structured illumination microscopy (SIM) was performed at 63x magnification on an ELYRA Super-Resolution Microscope (Carl Zeiss). 2.5µL of sample was pipetted to SecureSeal microchambers on microscope slides then cover-slipped. Droplet formation was first confirmed under 488nm and 594nm fluorescent LEDs. Then 488nm and 593nm laser lines were selected to perform z-stack imaging droplets (0.1µm z interval). Images were

processed with the default “Structural Illumination Processing Software”. Images are presented either as an orthogonal gallery or flattened as a maximum intensity projection image.

Recombinant hybrid RBPs

HIS-tagged hybrid RBPs were produced through InFusion (Takara) cloning, expression from the pET28a vector and purification as described above. The N-terminal RRMs of TIA1 (aa 1 to 289) were fused to the RGG domain of G3BP1 (aa 430 to 461) making [HIS::TIA1(RRMs)::G3BP1(RGG)] (predicted 35.1kDa), or the IDR of HNRNPA1 (aa 195 to 372) making [HIS::TIA1(RRMs)::HNRNPA1(IDR)] (predicted 46.4kDa) (**Supp. Figure S6C, D**). Construct of the reciprocal hybrids were also made: N-terminal of G3BP1 (aa 1 to 429) or RRMs of HNRNPA1 (aa 1 to 194) fused to the IDR of TIA1 (aa 290 to 386) making [HIS::G3BP1(N-term)::TIA1(IDR)] or [HIS::HNRNPA1(RRMs)::TIA1(IDR)]. However, we were unable to successfully purify recombinant hybrid RBPs containing the TIA1 IDR from bacterial cells.

Primary neuronal culture

All animals were housed and treated in accordance with Boston University IACUC protocols. Primary hippocampal neurons were isolated from P0 C57Bl/6J pups and cultured in neurobasal medium (Gibco) supplemented with 2% B-27 (Gibco), 200µM L-Glutamine and PenStrep. neurons were plated at $3x10^4$ cell/well onto 12mm poly-D-lysine-coated coverslips in 24 well plates, transduced at DIV2 with AAV1[0N4R wt tau::V5] or AAV1[EGFP] (MOI 200) and cultured with replenishment of media every third day. Human tau is expressed by AAV transduction to facilitate seeding of pathology following exposure to exogenous tau treatments. After 7 days *in vitro* (DIV), neurons were exposed to tau/TIA1 reacted samples (below) by careful removal of media and replacement with conditioned media into which treatments were diluted. For dose response, treatment concentrations were as follows: 1) tau 0.16µg/ml, HIS::TIA1 0.13µg/ml (or 4nM each monomer); 2) tau 0.8µg/ml, HIS::TIA1 0.67µg/ml (or 20nM each monomer); 3) tau 4µg/ml, HIS::TIA1 3.34µg/ml (or 100nM each monomer); 4) tau 20µg/ml, HIS::TIA1 16.7µg/ml (or 500nM each monomer).

The neurons were washed in PBS and then fixed in 4% paraformaldehyde in PBS (15 mins at 4°C). Fixed neurons were permeabilzed (10 mins at RT in PBS + 0.2% Tween-20), washed 3x in PBS, blocked in PBS + 2% normal donkey serum (1 hour at RT), washed 3x in PBS then immunolabelled overnight at 4°C with (chicken) anti-MAP2 (1:400, Aves) and (rabbit) anti-V5 (1:1000, Sigma) primary antibodies. The following day, neurons were washed 3x in PBS then incubated with (donkey) anti-rabbit-AF488 (1:800, Jackson Immuno) and (donkey) anti-chicken-AF647 (1:400, Jackson Immuno). Coverslips were washed 3x in PBS, counterstained with 0.5µg/ml DAPI, then mounted to slides on ProLong Gold antifade reagent (Thermo). Neurons were imaged at 20x on a Zeiss AxioObserver A1 epifluorescent microscope. Images were exported as tif files and imported into Imaris (BitPlane) software in which an unbiased mask was developed to quantify the number of DAPI stained nuclei within MAP2

positive cells, thereby counting neuronal cell number/field of view. Graphing and statistical comparisons were performed as indicated in GraphPad Prism.